THE JOURNAL OF PHYSICAL CHEMISTRY B

ARTICLE

pubs.acs.org/JPCB

Heat Capacities and Asymmetric Criticality of Coexistence Curves for Benzonitrile + Alkanes and Dimethyl Carbonate + Alkanes

Meijun Huang,[†] Yuntao Lei,[‡,§] Tianxiang Yin,[†] Zhiyun Chen,[†] Xueqin An,[†] and Weiguo Shen*[,†,‡]

[†]School of Chemistry and Molecular Engineering, East China University of Science and Technology, Shanghai 200237, China

[‡]Department of Chemistry, Lanzhou University, Lanzhou, Gansu 730000, China

Supporting Information

ABSTRACT: The critical behavior of isobaric heat capacities per unit volume for a series of critical binary solutions {benzonitrile + octane, or dodecane, or hexadecane} and {dimethyl carbonate + nonane, or decane, or dodecane} were studied. The corresponding exponent was obtained to be in consistent with the 3D-Ising value. The amplitudes in one-phase and two-phase regions were deduced, which were used to test some critical amplitude ratios. Analysis of the dependence of the effective critical exponent of the heat capacity on the temperature indicated a critical crossover from the 3D-Ising to the mean-field for all the studied systems. It was found that the heat capacity does play an important role for describing the asymmetric criticality of coexistence curves by the complete scaling theory.

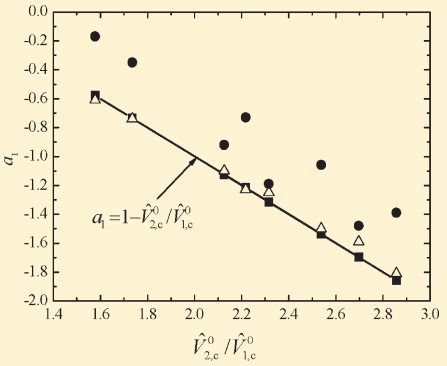

INTRODUCTION

The asymmetric criticality of coexistence curves has been paid much attention recently. A few years ago, Fisher and co-workers[1,2] proposed a general formulation of complete scaling for one-component fluids, which showed that the three scaling fields should be the linear mix of all physical fields: not only the chemical potential and the temperature but also the pressure. It was concluded that the strong singularity of the diameter of coexistence curves was a consequence of the complete scaling. Recently, Anisimov et al.[3−5] extended the complete scaling to binary solutions for both incompressible and weakly compressible liquid mixtures. According to the theory proposed by Anisimov and co-workers,[4,5] the width ΔZ_{cxc} and the diameter Z_{d} of a coexistence curve can be expressed by

$$\Delta Z_{\mathrm{cxc}} \equiv |Z^{\mathrm{U}} - Z^{\mathrm{L}}|/2 \approx \pm \hat{B}_0^Z|\tau|^{\beta}(1 + \hat{B}_1^Z|\tau|^{\Delta} + \hat{B}_2^Z|\tau|^{2\beta}) \quad (1)$$

$$Z_{\mathrm{d}} \equiv (Z^{\mathrm{U}} + Z^{\mathrm{L}})/2 \approx Z_{\mathrm{c}} + \hat{D}_2^Z|\tau|^{2\beta} + \hat{D}_1^Z\left(\frac{\hat{A}^-}{1-\alpha}|\tau|^{1-\alpha} + \hat{B}_{\mathrm{cr}}|\tau|\right) \quad (2)$$

where Z is the physical density, such as the mole fraction x_2 of component 2, the reduced density $\hat{\rho}$ ($\hat{\rho} = \rho/\rho_{\mathrm{c}} = V_{\mathrm{c}}/V$, where ρ and V are the molar density and the molar volume of the binary solution, respectively), and the reduced partial molar density of component 2, $\hat{\rho}x_2$ (the product of $\hat{\rho}$ and x_2); the subscript c denotes their critical values; the superscripts "U" and "L" refer to upper and lower phases, respectively; $\hat{B}_0^z$, $\hat{B}_1^z$, $\hat{B}_2^z$, $\hat{D}_2^z$, and $\hat{D}_1^z$ are the system dependent amplitudes; β, α, and Δ are the critical exponents relating to the width of the coexistence curve, the heat capacity, and the first Wegner correction term; $\hat{B}_{\mathrm{cr}} = B_{\mathrm{cr}}V_{\mathrm{c}}/R$ is a reduced variable with B_{cr} being the critical fluctuation-induced contribution to the background of the heat capacity and R being the gas constant; $\hat{A}^- = A^-V_{\mathrm{c}}/\alpha R$ is a reduced variable with A^- being the critical amplitude relating to the heat capacity in the two-phase region; and $\tau = |T - T_{\mathrm{c}}|/T_{\mathrm{c}}$ is the reduced temperature with T_{c} being the critical temperature.

According to eqs 1 and 2, a test of the complete scaling requires both coexisting-curve data and heat capacity data for a series of binary solutions. However, for lack of the precise heat capacity data in a wide temperature range, the test was done with the assumption that the second term of eq 2 for $Z = x_2$ was negligible, or was replaced by the apparent term of $|\tau|^{1-\alpha}$ for $Z = \hat{\rho}x_2$ and $Z = \hat{\rho}$.[5]

In order to evaluate the effect of heat capacity on the asymmetry of liquid−liquid coexistence curve, in this paper, we measure heat capacities for a series of critical binary solutions {benzonitrile + octane, or dodecane, or hexadecane} and {dimethyl carbonate + nonane, or decane, or dodecane} over the temperature

Received: July 6, 2011
Revised: September 16, 2011
Published: September 27, 2011

Table 1. Critical Mole Fractions and Critical Temperatures for {Benzonitrile + Alkanes} and {Dimethyl Carbonate + Alkanes}

system	$x_{2,c}$ (visual method)	$x_{2,c}$ (fitting by eq 22)	T_c/K (visual method)	T_c/K (calorimetry)
BN[a] + C8[b]	0.536[c]	0.538	283.225[c]	281.892
BN[a] + C9[d]	0.503[e]	0.503	284.625[e]	284.264
BN[a] + C12[f]	0.414[g]	0.416	293.028[g]	293.077
BN[a] + C14[h]	0.367[i]	0.364	298.858[i]	298.843
BN[a] + C16[j]	0.327[k]	0.324	304.408[k]	304.346
DMC[l] + C9[d]	0.337[m]	0.340	281.078[m]	281.548
DMC[l] + C10[n]	0.309[o]	0.311	287.102[o]	287.498
DMC[l] + C12[f]	0.261[m]	0.265	298.069[m]	298.364

[a] Benzonitrile. [b] Octane. [c] Reference 12. [d] Nonane. [e] Reference 6. [f] Dodecane. [g] Reference 9. [h] Tetradecane. [i] Reference 7. [j] Hexadecane. [k] Reference 11. [l] Dimethyl carbonate. [m] Reference 10. [n] Decane. [o] Reference 8.

range both near and far away from the critical points. The experimental results together with the previously reported heat capacities[6,7] for the systems {benzonitrile + tetradecane, or nonane} and the coexistence-curve data for the above eight systems[6−12] are fitted by simplified eqs 1 and 2 to obtain the corresponding coefficients, which are used to analyze the asymmetry of the coexistence curves and evaluate the contribution of the heat capacity.

EXPERIMENTAL SECTION

Chemicals. Benzonitrile, octane, nonane, decane, dodecane, and hexadecane were supplied by Alfa Aesar. Dimethyl carbonate was purchased from ABCR GmbH & Co, KG. All the chemicals had the mass fraction of 0.99, and were dried and stored over freshly activated 0.4 nm molecular sieves.

Apparatus and Procedure. A series of critical binary solutions of {benzonitrile + octane, or dodecane, or hexadecane} and {dimethyl carbonate + nonane, or decane, or dodecane} were prepared by weighing, and the uncertainty in determination of the mole fraction of benzonitrile (or dimethyl carbonate) is better than ±0.001. In this paper, we define the pure component with the larger molar volume as component 2, thus x_2 is the mole fraction of alkane. The critical mole fractions of $x_{2,c}$ for all the systems under studying were determined previously,[6−12] which are listed in Table 1.

The isobaric heat capacity per unit volume C_pV^{-1} was measured by using a Setaram Micro DSC III differential scanning calorimeter, which is based on the Tian-Calvet's principle. This calorimeter affords convenient operation over a wide temperature range with a small amount of sample (about 1 cm^3). Setaram liquid heat capacity vessels were used in our measurements, which avoided the presence of the vapor phase over the liquid, thus no vapor phase correction was needed.[13] The background noise of Micro DSC III was less than ±0.2 μw, and the temperature stability was better than ±0.002 K.

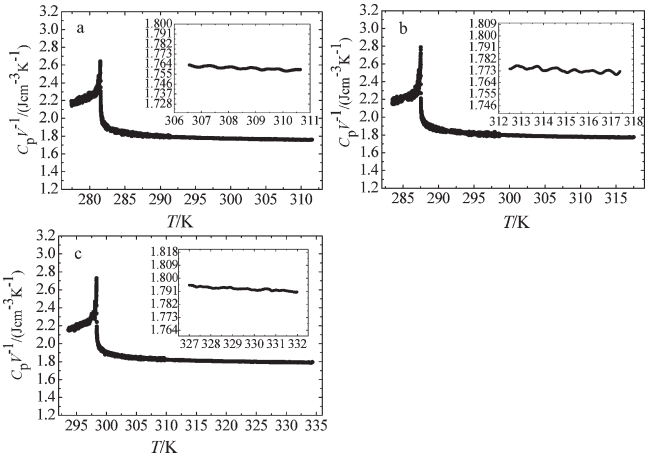

Figure 1. Isobaric heat capacities per unit volume (C_pV^{-1}) for the critical binary solutions (a) dimethyl carbonate + nonane, (b) dimethyl carbonate + decane, and (c) dimethyl carbonate + dodecane. Each inset figure shows the linear dependence of C_pV^{-1} on temperature in the range far away from the critical point.

The isobaric heat capacities per unit volume C_pV^{-1} for a series of critical binary solutions of {benzonitrile + octane, or dodecane, or hexadecane} and {dimethyl carbonate + nonane, or decane, or dodecane} were determined by three measurements. In each measurement, the reference vessel was always filled with heptane, while the measuring vessel was filled with heptane, 1-butanol, and the sample to be investigated, respectively. All three measurements were performed in the down scanning model at ambient pressure. By carefully examining the effects of scanning rate on the uncertainties of measurements, and balancing the time consumption and the thermal delay, the proper scanning rate was selected to be 0.01 K min^{-1} and 0.1 K min^{-1} for the critical region and the temperature range away from the critical region, respectively.

The isobaric heat capacity per unit volume $(C_pV^{-1})_s$ of the sample investigated was calculated by

$$(C_pV^{-1})_s = (C_pV^{-1})_0 + ((C_pV^{-1})_r - (C_pV^{-1})_0)\cdot((HF_s - HF_0)/(HF_r - HF_0)) \quad (3)$$

where HF_0, HF_r, and HF_s are the heat flow of heptane, 1-butanol, and the sample, respectively; $(C_pV^{-1})_0$ and $(C_pV^{-1})_r$ are the isobaric heat capacities per unit volume of heptane and 1-butanol, respectively, which can be calculated by isobaric molar heat capacities $C_{p,m}$ and densities ρ though $C_pV^{-1} = C_{p,m}\rho/M$ with M being the molar mass. The isobaric molar heat capacities $C_{p,m}$ and the densities ρ for heptane and 1-butanol were taken from the literature.[14−16] The corresponding uncertainties in the C_pV^{-1} measurements were estimated to be less than ±0.001 J cm^{-3} K^{-1} over the temperature range away from the critical point and ±0.01 J cm^{-3} K^{-1} in the critical region, except for the immediate vicinity of the critical point, where the heat capacity is very sensitive to the temperature change. An additional systematic uncertainty was introduced by the uncertainties of isobaric heat capacities per unit volume of the two reference samples heptane and 1-butanol, which was estimated to be about ±0.002 J cm^{-3} K^{-1}. More detailed description of the apparatus and the principle of

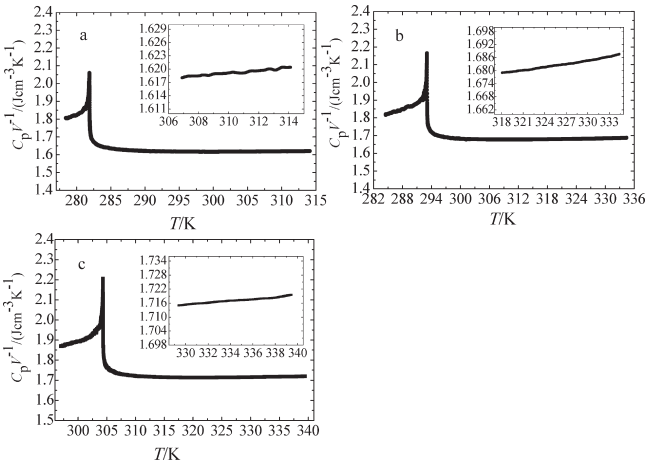

Figure 2. Isobaric heat capacities per unit volume (C_pV^{-1}) for the critical binary solutions: (a) benzonitrile + octane; (b) benzonitrile + dodecane; (c) benzonitrile + hexadecane. Each inset figure shows the linear dependence of C_pV^{-1} on temperature in the range far away from the critical point.

the measurement could be found in our previously published article.[6]

RESULTS AND DISCUSSION

Analysis of the Experimental Heat Capacity Data. The isobaric heat capacities per unit volume C_pV^{-1} of critical binary solutions {benzonitrile + octane, or dodecane, or hexadecane} and {dimethyl carbonate + nonane, or decane, or dodecane} were determined in a wide temperature range of $-8\ \mathrm{K} \leq T - T_c \leq 30\ \mathrm{K}$. About 10 000−30 000 data were collected for each solution and summarized as the Supporting Information. Figures 1 and 2 illustrate the dependence of C_pV^{-1} on temperature for above six systems with the insets showing the dependence on temperature far away from the critical points.

The critical behavior of the isobaric heat capacity per unit volume may be described by

$$C_pV^{-1} = C_{p0} + E\tau + \frac{A^+}{\alpha}|\tau|^{-\alpha}(1 + D^+|\tau|^{\Delta} + \cdots) \quad \text{the homogeneous phase} \quad (4)$$

$$C_pV^{-1} = C_{p0} + E\tau + \frac{A^-}{\alpha}|\tau|^{-\alpha}(1 + D^-|\tau|^{\Delta} + \cdots) \quad \text{the heterogeneous phase} \quad (5)$$

where the theoretical values of the exponents α and Δ are accepted to be 0.110[17,18] and 0.50,[19,20] respectively; D^+ and D^- are the amplitudes of the first correction-to-scaling term; A^+ and A^- are the amplitudes of the leading divergence of the isobaric heat capacity per unit volume, where the plus sign denotes the homogeneous phase, and the minus sign denotes the heterogeneous phase; the analytical term C_{p0} contains two components: $C_{p0} = B_{bg} + B_{cr}$, with B_{bg} being a true background heat capacity far away from the critical point, and B_{cr} being a critical-fluctuation induced contribution to the background heat capacity; and $E\tau$ is the linear background term arising from the regular part of the free energy. C_{p0}, E, α, and Δ are predicted to be the same above and below the critical point.[21] Although A^+ and A^- are not universal and depend on the microscopic characteristics of the system, the value of the ratio A^+/A^- is a universal quantity and was predicted to be 0.537 ± 0.019 by $d = 3$ expansion,[22] 0.530 ± 0.003 by high-temperature series,[23,24] 0.527 ± 0.037 by ε expansion,[22] and 0.55 ± 0.01 by Monte Carlo simulation.[25]

Table 2. The Values of Background Isobaric Heat Capacity per Unit Volume Far Away from the Critical Temperature B_{bg} and the Coefficients of the Linear Background Term of Isobaric Heat Capacity Per Unit Volume E for {Benzonitrile + Akanes} and {Dimethyl Carbonate + Alkanes}

system	B_{bg}/(J cm^{-3} K^{-1})	E/(J cm^{-3} K^{-1})
BN[a] + C8[b]	1.6107 ± 0.0005	0.084 ± 0.001
BN[a] + C9[c]	1.6256 ± 0.0004[d]	0.122 ± 0.001[d]
BN[a] + C12[e]	1.6659 ± 0.0005	0.150 ± 0.001
BN[a] + C14[f]	1.6868 ± 0.0005[g]	0.149 ± 0.001[g]
BN[a] + C16[h]	1.7053 ± 0.0005	0.119 ± 0.001
DMC[i] + C9[c]	1.7867 ± 0.0005	−0.276 ± 0.005
DMC[i] + C10[j]	1.8063 ± 0.0008	−0.344 ± 0.009
DMC[i] + C12[e]	1.8161 ± 0.0003	−0.225 ± 0.003

[a] Benzonitrile. [b] Octane. [c] Nonane. [d] Reference 6. [e] Dodecane. [f] Tetradecane. [g] Reference 7. [h] Hexadecane. [i] Dimethyl carbonate. [j] Decane.

In order to analyze the critical behavior of the isobaric heat capacity per unit volume of a critical binary solution, it is necessary to determine its critical temperature. However, the liquid heat capacity vessel used in our measurements is made of metal, therefore it is impossible to determine the critical temperature by the traditional visual method, and an alternative procedure then was used to determine the critical temperature.[6,7] As shown in Figures 1 and 2, there exists a sharp peak for each heat capacity curve, and the temperature corresponding to the highest value of the heat capacity may be roughly taken as the critical point, within ±3 K from which the term of $|\tau|^{-\alpha}$ was found to be dominant and the correction-to-scaling terms are negligible.[6,27] Thus first, we set the temperature corresponding to the highest value of measured heat capacity as an approximation of the critical one and fitted the experimental data to eqs 4 and 5 with $D^+ = D^- = 0$, and the standard deviation of the fit was calculated. This procedure was repeated for a series of temperatures within the range of ±3 K from the maximum point with a step of 0.001 K and a minimum standard deviation of the fit was found, at which the corresponding temperature was accepted as the critical one. The results are shown and compared with those determined by the traditional visual method in Table 1. There are some differences between the critical temperatures determined by the calorimetry and those obtained from the visual method, which can be attributed to the different sources of the chemicals, and the uncontrollable moisture and impurities introduced during the preparation of the critical binary solutions.

As is shown in the insets of Figures 1 and 2, in the one-phase region far away from the critical points, the isobaric heat capacity per unit volume C_pV^{-1} shows a linear dependence on the temperature T, which can be described by the following equation:

$$C_pV^{-1} = B_{bg} + E\tau \quad (6)$$

Table 3. Critical Parameters in eqs 4 and 5 for {Benzonitrile + Akanes}

temperature range	C_{p0} Jcm^{-3}K^{-1}	A^+ Jcm^{-3}K^{-1}	A^- Jcm^{-3}K^{-1}	α	Δ	A^+/A^-	$D^+ = D^-$
			benzonitrile + octane				
$\lvert T - T_c\rvert \leq 3$ K	1.446 ± 0.001	0.0129 ± 0.0001	0.0241 ± 0.0001	0.108 ± 0.001		(0.53)[a]	(0)[a]
$\lvert T - T_c\rvert \leq 3$ K	1.443 ± 0.001	0.0128 ± 0.0001	0.0240 ± 0.0001	(0.110)[a]		0.533 ± 0.001	(0)[a]
0 K < $(T - T_c) \leq 3$ K	1.426 ± 0.001	0.0139 ± 0.0001		(0.110)[a]			(0)[a]
0 K < $(T - T_c) \leq 15$ K	(1.426)[a]	0.0134 ± 0.0001		(0.110)[a]	(0.50)[a]		0.42 ± 0.01
			benzonitrile + dodecane				
$\lvert T - T_c\rvert \leq 3$ K	1.500 ± 0.001	0.0130 ± 0.0002	0.0245 ± 0.0001	0.109 ± 0.001		(0.53)[a]	(0)[a]
$\lvert T - T_c\rvert \leq 3$ K	1.499 ± 0.001	0.0129 ± 0.0001	0.0243 ± 0.0001	(0.110)[a]		0.531 ± 0.002	(0)[a]
0 K < $(T - T_c) \leq 3$ K	1.486 ± 0.001	0.0137 ± 0.0001		(0.110)[a]			(0)[a]
0 K<$(T-T_c)\leq$15 K	(1.486)[a]	0.0133 ± 0.0001		(0.110)[a]	(0.50)[a]		0.37 ± 0.01
			benzonitrile + hexadecane				
$\lvert T - T_c\rvert \leq 3$ K	1.533 ± 0.001	0.0130 ± 0.0002	0.0245 ± 0.0001	0.111 ± 0.001		(0.53)[a]	(0)[a]
$\lvert T - T_c\rvert \leq 3$ K	1.529 ± 0.001	0.0133 ± 0.0001	0.0249 ± 0.0001	(0.110)[a]		0.534 ± 0.002	(0)[a]
0 K < $(T - T_c) \leq 3$ K	1.525 ± 0.001	0.0135 ± 0.0001		(0.110)[a]			(0)[a]
0 K < $(T - T_c) \leq 15$ K	(1.525)[a]	0.0133 ± 0.0001		(0.110)[a]	(0.50)[a]		0.27 ± 0.01

[a] The values in the bracket were fixed in the fitting.

Table 4. Critical Parameters in eqs 4 and 5 for {Dimethyl Carbonate + Alkanes}

temperature range	C_{p0} Jcm^{-3}K^{-1}	A^+ Jcm^{-3}K^{-1}	A^- Jcm^{-3}K^{-1}	α	Δ	A^+/A^-	$D^+ = D^-$
			dimethyl carbonate + nonane				
$\lvert T - T_c\rvert \leq 3$ K	1.473 ± 0.002	0.0264 ± 0.0002	0.0499 ± 0.0003	0.101 ± 0.001		(0.53)[a]	(0)[a]
$\lvert T - T_c\rvert \leq 3$ K	1.500 ± 0.004	0.0236 ± 0.0003	0.0456 ± 0.0003	(0.110)[a]		0.518 ± 0.003	(0)[a]
0 K < $(T - T_c) \leq 3$ K	1.396 ± 0.004	0.0230 ± 0.0002		(0.110)[a]			(0)[a]
0 K < $(T - T_c) \leq 15$ K	(1.396)[a]	0.0290 ± 0.0001		(0.110)[a]	(0.50)[a]		0.34 ± 0.01
			dimethyl carbonate + decane				
$\lvert T - T_c\rvert \leq 3$ K	1.499 ± 0.002	0.0245 ± 0.0002	0.0462 ± 0.0003	0.108 ± 0.001		(0.53)[a]	(0)[a]
$\lvert T - T_c\rvert \leq 3$ K	1.496 ± 0.005	0.0244 ± 0.0003	0.0457 ± 0.0003	(0.110)[a]		0.533 ± 0.003	(0)[a]
0 K < $(T - T_c) \leq 3$ K	1.445 ± 0.005	0.0273 ± 0.0003		(0.110)[a]			(0)[a]
0 K<$(T-T_c)\leq$15 K	(1.445)[a]	0.0268 ± 0.0001		(0.110)[a]	(0.50)[a]		0.28 ± 0.01
			dimethyl carbonate + dodecane				
$\lvert T - T_c\rvert \leq 3$ K	1.523 ± 0.001	0.0230 ± 0.0002	0.0433 ± 0.0004	0.104 ± 0.001		(0.53)[a]	(0)[a]
$\lvert T - T_c\rvert \leq 3$ K	1.543 ± 0.003	0.0233 ± 0.0002	0.0430 ± 0.0002	(0.110)[a]		0.519 ± 0.007	(0)[a]
0 K < $(T - T_c) \leq 3$ K	1.499 ± 0.003	0.0248 ± 0.0002		(0.110)[a]			(0)[a]
0 K < $(T - T_c) \leq 15$ K	(1.499)[a]	0.0247 ± 0.0001		(0.110)[a]	(0.50)[a]		0.14 ± 0.01

[a] The values in the bracket were fixed in the fitting.

Thus, by fitting the experimental data with eq 6, the values of B_{bg} and E were obtained, which are summarized in Table 2. The values of E then were fixed in all the following analysis procedures.

It is almost impossible to fit the experimental data to eqs 4 and 5 with all the parameters being adjustable for determining the critical exponent α and the amplitude ratio A^+/A^- simultaneously, because of the strong correlation among the parameters, particularly between the critical exponent α and the amplitude A^+ or A^-. Therefore, in the following analysis procedures, T_c and E were set as the values determined from the methods mentioned above and all experimental data in the region of ±3 K from the critical temperature were fitted to eqs 4 and 5 with the critical exponent α or the amplitude ratio being fixed at their theoretical values: $\alpha = 0.110$, or $A^+/A^- = 0.53$, while the first correction to the scaling term was neglected, namely $D^+ = D^- = 0$. The results of the fits are shown in Table 3 and Table 4. The values of the critical exponent α or the amplitude ratio A^+/A^- determined in this procedure are consistent with the theoretical values.

One of the disadvantages of Micro DSC III is that it can not afford stirring, which is of great importance in the measurement of the heat capacity in the two-phase region, while it can be negligible in the one-phase region. Thus, the data in the one-phase region are much more reliable than those in the two-phase region. Therefore, we fitted only the experimental data in a temperature range of 0 K < $(T - T_c) \leq 3$ K to eq 4 with T_c and E being fixed at the values obtained above, α being fixed at its theoretical value 0.110, and $D^+ = D^- = 0$. The fitting results of A^+ and C_{p0} are listed in Tables 3 and 4.

dx.doi.org/10.1021/jp206380t |J. Phys. Chem. B 2011, 115, 13608–13616

Table 5. The Critical-Fluctuation-Induced Contribution to the Background Heat Capacity B_{cr} and Its Reduced Variable $\hat{B}_{cr}$, the Critical Amplitude of Correlation Length ξ_0^+, Amplitude Ratio $R_{B_{cr}}^+$, and Reduced Critical Amplitude $\hat{A}^-$ of the Isobaric Heat Capacity per Unit Volume in the Two-Phase Region for {Benzonitrile + Akanes} and {Dimethyl Carbonate + Alkanes}

system	$B_{cr}/(\mathrm{Jcm^{-3}K^{-1}})$	$\hat{B}_{cr}$	$\xi_0^+/(\mathrm{nm})$ this work	$\xi_0^+/(\mathrm{nm})$ reference	$R_{B_{cr}}^+$	$\hat{A}^-$
BN[a] + C8[b]	−0.185 ± 0.001	−2.969	0.267 ± 0.001	0.270[c]	−0.55 ± 0.01	3.818
BN[a] + C9[d]	−0.179 ± 0.001[e]	−3.008		0.268[e]	−0.467[e]	3.936
BN[a] + C12[f]	−0.180 ± 0.001	−3.340	0.268 ± 0.001	0.271[g]	−0.54 ± 0.01	4.345
BN[a] + C14[h]	−0.184 ± 0.001[i]	−3.567		0.275[i]	−0.513[i]	4.609
BN[a] + C16[j]	−0.180 ± 0.001	−3.602	0.269 ± 0.001	0.269[k]	−0.50 ± 0.01	4.645
DMC[l] + C9[d]	−0.391 ± 0.004	−5.383	0.228 ± 0.001	0.212[m]	−0.53 ± 0.01	5.427
DMC[l] + C10[n]	−0.361 ± 0.004	−5.107	0.215 ± 0.001	0.215[m]	−0.51 ± 0.01	6.627
DMC[l] + C12[f]	−0.317 ± 0.003	−4.662	0.222 ± 0.001	0.214[o]	−0.46 ± 0.01	6.255

[a] Benzonitrile. [b] Octane. [c] Reference 12. [d] Nonane. [e] Reference 6. [f] Dodecane. [g] Reference 9. [h] Tetradecane. [i] Reference 7. [j] Hexadecane. [k] Reference 11. [l] Dimethyl carbonate. [m] Reference 27. [n] Decane. [o] Reference 28.

Substituting the values of A^+ into the two-scale-factor universality ratio $X = A^+(\xi_0^+)^3/k_B$ (k_B is the Boltzmann constant), and fixing X at its theoretical prediction value 0.01966 ± 0.00017[26] for $d = 3$ expansion, the values of the amplitude of correlation length ξ_0^+ were calculated, which are summarized in Table 5. As it can be seen from Table 5, the values of ξ_0^+ are in agreement with the literature ones.[9,11,12,27,28] In addition, the values of B_{cr} were obtained by subtraction of B_{bg} from C_{p0}, which are also listed in Table 5.

By using the values of C_{p0} obtained above, we fitted the experimental data by eq 4 in a wider temperature range of ($0\ \mathrm{K} < (T - T_c) \leq 15\ \mathrm{K}$), where the correction to scaling terms become somewhat significant, with T_c and E being fixed at the values obtained above, and α and Δ being fixed at theoretical values 0.110 and 0.50, respectively. We determined A^+ and D^+, and the results are also listed in Tables 3 and 4.

Bagnuls and Bervillier introduced an amplitude ratio[21,29]

$$R_{B_{cr}}^+ = (A^+/\alpha)|D^+|^{\alpha/\Delta}/B_{cr} \quad (7)$$

correlating the critical part of the background heat capacity B_{cr}, the amplitude A^+ and the amplitude D^+, and proposed a universal value of $R_{B_{cr}}^+$ of −0.708.[30] Anisimov and Kiselev proposed another expression for $R_{B_{cr}}^+$:[31]

$$R_{B_{cr}}^+ = -R_0(1-u)^{\alpha/\Delta} \quad (8)$$

where u is a coupling constant, and R_0 is a universal number, which can be calculated by

$$R_0 = \frac{1}{2}(2-\alpha)(1-\alpha)\left(\frac{2\alpha(2-\alpha+\Delta)(1-\alpha+\Delta)}{(2-\alpha)(1-\alpha)}\right)^{\alpha/\Delta} \quad (9)$$

$R_0 = 0.704$ is a constant. In the infinite-cutoff limit, u is zero and eq 8 becomes universal. We calculated the values of $R_{B_{cr}}^+$ from eq 7 by using the experimentally determined A^+, D^+ and B_{cr}, which are listed in Table 5. They are consistent with those determined by other researchers,[31−34] but significantly smaller than the prediction of Bagnuls. As commonly accepted, the value of u in eq 8 varies from 0.4 to 0.9 for simple fluids and fluid mixtures, which gives $R_{B_{cr}}^+$ from 0.43 to 0.63. Thus, the values of $R_{B_{cr}}^+$ calculated from our experimental critical amplitudes are in reasonable agreement with those predicted by Anisimov.[31]

As is shown in Figures 1 and 2, the singular behavior of the heat capacity is dominate only in the temperature range close to the critical point, and as the temperature is far away from the critical point, the regular behavior of the heat capacity becomes more and more prominent, which exhibits a behavior of crossover to mean-field class. We defined an effective critical exponent $\alpha_{eff} = -d\ln(C_pV^{-1} - C_{p0} - E\tau)/d\ln\tau$ to describe the crossover behavior of heat capacity, whose values at various temperatures were obtained by a spline fit of all the experimental data in the one-phase region, with T_c, E, and B_{cr} being fixed at the values obtained above, and C_{p0} being fixed at the values obtained from the fit of the experimental data in the one-phase region using eq 4. As an example, Figure 3 shows such a crossover from 3D-Ising to the mean-field one for binary solution {dimethyl carbonate + decane}. It clearly shows in Figure 3 that the value of α_{eff} decreases from about 0.11 near the critical point to almost zero in the temperature range far away from the critical point.

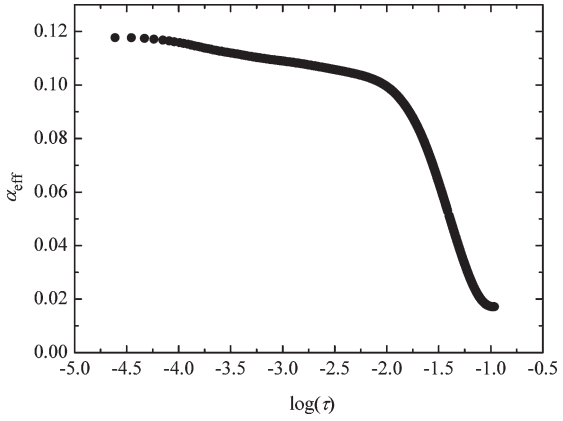

Figure 3. Effective critical exponent a_{eff} of isobaric heat capacity per unit volume as a function of log(τ) for {dimethyl carbonate + decane}.

Complete Scaling Theory in Binary Solutions. According to the theory proposed by Anisimov,[4,5] the strongly fluctuating scaling density and the weakly fluctuating scaling density may be described by $\varphi_1 = (\partial h_3/\partial h_1)_{h_2}$ and $\varphi_2 = (\partial h_3/\partial h_2)_{h_1}$, respectively; and the strong scaling field h_1, the weak scaling field h_2, and the dependent scaling field h_3 are expressed as the linear mix of the physical fields $\Delta\hat{\mu}_1$, $\Delta\hat{\mu}_{21}$, $\Delta\hat{T}$, and $\Delta\hat{P}$:

$$h_1 = \Delta\hat{\mu}_{21} + a_1\Delta\hat{\mu}_1 + a_2\Delta\hat{T} + a_3\Delta\hat{P} \quad (10)$$

$$h_2 = \Delta\hat{T} + b_2\Delta\hat{\mu}_1 + b_3\Delta\hat{P} + b_4\Delta\hat{\mu}_{21} \quad (11)$$

$$h_3 = \Delta\hat{P} - \Delta\hat{\mu}_1 - \hat{S}_c\Delta\hat{T} - x_{2,c}\Delta\hat{\mu}_{21} \quad (12)$$

Table 6. The Critical Amplitudes $\hat{D}_1^{\hat{\rho}}$, $\hat{D}_1^{\hat{\rho}x_2}$, $\hat{D}_2^{x_2}$, $\hat{B}_0^{x_2}$, and $\hat{B}_0^{\hat{\rho}}$ for {Benzonitrile + Alkanes} and {Dimethyl Carbonate + Alkanes}

system	$\hat{D}_1^{\hat{\rho}}$	$\hat{D}_1^{\hat{\rho}x_2}$	$\hat{D}_1^{x_2}$	$\hat{D}_2^{x_2}$	$\hat{B}_0^{x_2}$	$\hat{B}_0^{\hat{\rho}}$
BN[a] + C8[b]	0.162 ± 0.003	−0.111 ± 0.004	−0.198 ± 0.005	0.276 ± 0.004	0.777 ± 0.009	−0.343 ± 0.004
BN[a] + C9[c]	0.156 ± 0.002	−0.080 ± 0.004	−0.158 ± 0.004	0.346 ± 0.004	0.802 ± 0.002	−0.431 ± 0.001
BN[a] + C12[d]	0.181 ± 0.003	−0.066 ± 0.002	−0.141 ± 0.003	0.515 ± 0.004	0.796 ± 0.003	−0.637 ± 0.002
BN[a] + C14[e]	0.166 ± 0.004	−0.044 ± 0.003	−0.104 ± 0.004	0.584 ± 0.006	0.776 ± 0.003	−0.753 ± 0.002
BN[a] + C16[f]	0.162 ± 0.002	−0.033 ± 0.002	−0.085 ± 0.003	0.635 ± 0.005	0.746 ± 0.003	−0.843 ± 0.001
DMC[g] + C9[c]	0.131 ± 0.006	−0.027 ± 0.007	−0.072 ± 0.008	0.590 ± 0.009	0.858 ± 0.002	−0.689 ± 0.001
DMC[g] + C10[h]	0.066 ± 0.003	0.008 ± 0.003	−0.013 ± 0.004	0.620 ± 0.006	0.830 ± 0.001	−0.755 ± 0.001
DMC[g] + C12[d]	0.082 ± 0.003	0.001 ± 0.002	−0.021 ± 0.003	0.665 ± 0.005	0.771 ± 0.002	−0.867 ± 0.001

[a] Benzonitrile. [b] Octane. [c] Nonane. [d] Dodecane. [e] Tetradecane. [f] Hexadecane. [g] Dimethyl carbonate. [h] Decane.

where $\mu_{21} \equiv \mu_2 - \mu_1$, with μ_1 and μ_2 being the chemical potential of component 1 (solvent) and component 2 (solute); $\Delta\hat{T} \equiv (T - T_c)/T_c$, $\Delta\hat{P} \equiv (P - P_c)/(\rho_c RT_c)$, $\Delta\hat{\mu}_1 \equiv (\mu_1 - \mu_{1,c})/RT_c$, $\Delta\hat{\mu}_{21} \equiv (\mu_{21} - \mu_{21,c})/(RT_c)$, and $\hat{S}_c = S_c/R$ are the reduced temperature, the reduced pressure, the reduced chemical potential of component 1, the reduced chemical-potential difference between the two components, and the reduced critical molar entropy (S is the molar entropy of the solution); subscript "c" indicates the critical value; a_i and b_i are system dependent coefficients. From the hypothesis that the theoretical scaling fields are the linear mix of the physical ones, eqs 1 and 2 may be deduced. The system-dependent amplitudes $\hat{B}_0^z$, $\hat{B}_2^z$, $\hat{D}_2^z$, and $\hat{D}_1^z$ in eqs 1 and 2 can be expressed for Z being x_2, $\hat{\rho}$, and $\hat{\rho}x_2$, respectively, by

$$\hat{B}_0^{x_2} = (1 - a_1 x_{2,c})B_0|\tau_0|^\beta, \quad \hat{B}_0^{\hat{\rho}} = (a_1 + a_3)B_0|\tau_0|^\beta$$
$$\hat{B}_0^{\hat{\rho}x_2} = (1 + a_3 x_{2,c})B_0|\tau_0|^\beta \tag{13}$$

$$\hat{B}_2^{x_2} = \frac{a_1^2(\hat{B}_0^{x_2})^2}{(1 - a_1 x_{2,c})^2}, \quad \hat{B}_2^{\hat{\rho}} = \frac{a_1^2(\hat{B}_0^{\hat{\rho}})^2}{(a_1 + a_3)^2}$$
$$\hat{B}_2^{\hat{\rho}x_2} = \frac{a_3^2(\hat{B}_0^{\hat{\rho}x_2})^2}{(1 + a_3 x_{2,c})^2} \tag{14}$$

$$\hat{D}_2^{x_2} = -\frac{a_1(\hat{B}_0^{x_2})^2}{1 - a_1 x_{2,c}}, \quad \hat{D}_2^{\hat{\rho}} = \frac{a_3(\hat{B}_0^{\hat{\rho}})^2}{a_1 + a_3}$$
$$\hat{D}_2^{\hat{\rho}x_2} = \frac{a_3(\hat{B}_0^{\hat{\rho}x_2})^2}{1 + a_3 x_{2,c}} \tag{15}$$

$$\hat{D}_1^{x_2} = (b_2 x_{2,c} - b_4)|\tau_0|^{-1}, \quad \hat{D}_1^{\hat{\rho}} = -(b_2 + b_3)|\tau_0|^{-1}$$
$$\hat{D}_1^{\hat{\rho}x_2} = -(b_4 + b_3 x_{2,c})|\tau_0|^{-1} \tag{16}$$

With the assumption that the excess volume is negligible, the asymmetric coefficients a_1 and a_3 have the following relation:

$$a_3 \approx (1 - a_1)\hat{V}_{1,c}^0 - \hat{V}_{2,c}^0 \tag{17}$$

where $\hat{V}_{1,c}^0 = V_{1,c}^0/V_c$, $\hat{V}_{2,c}^0 = V_{2,c}^0/V_c$, $V_{1,c}^0$, and $V_{2,c}^0$ are molar volumes of the pure solvent and the pure solute at the critical temperature of the critical binary solution, respectively. V_c is the molar volume of the binary solution at the critical point.

Most of the values of a_3 calculated by Perez-Sanchez[5] from the available coexistence-curve data of binary solutions consisting of a polar solvent and an n-alkane were less than 0.3 and thought to be nearly vanishing. When we fitted our experimental coexistence-curve data with eq 2 to obtain $\hat{D}_1^{\hat{\rho}}$ and $\hat{D}_2^{\hat{\rho}}$ for $Z = \hat{\rho}$ or $\hat{D}_1^{\hat{\rho}x_2}$ and $\hat{D}_2^{\hat{\rho}x_2}$ for $Z = \hat{\rho}x_2$, we found that the correlation between $\hat{D}_1^{\hat{\rho}}$ and $\hat{D}_2^{\hat{\rho}}$, or $\hat{D}_1^{\hat{\rho}x_2}$ and $\hat{D}_2^{\hat{\rho}x_2}$ was as large as 99%, and the uncertainty for the adjusting parameters was possibly as large as 100% of the value, which possibly yielded an artificially large a_3. Therefore we prefer to use the incompressible hypothesis ($a_3 = 0$) in the following data analysis, hence the asymmetric coefficient a_1 may be deduced as a simple linear function of the solute/solvent reduced molar volume ratio $\hat{V}_{2,c}^0/\hat{V}_{1,c}^0$:[5]

$$a_1 \approx 1 - \hat{V}_{2,c}^0/\hat{V}_{1,c}^0 \tag{18}$$

In data analysis of the coexistence curves of the binary solutions reported in the literature,[5] the $\hat{D}_1^{x_2}$ term was neglected and eq 2 becomes a linear function of $|\tau|^{2\beta}$:

$$(x_2)_d \equiv \frac{x_2^U + x_2^L}{2} \approx x_{2,c} + \hat{D}_2^{x_2}|\tau|^{2\beta} \tag{19}$$

However, it is easy to see that the three equations of eq 16 are not all independent; they have the relation

$$\hat{D}_1^{x_2} = \hat{D}_1^{\hat{\rho}x_2} - \hat{D}_1^{\hat{\rho}}x_{2,c} \tag{20}$$

Thus, in principle, as long as $\hat{D}_1^{\hat{\rho}}$ and $\hat{D}_1^{\hat{\rho}x_2}$ are not negligible, the $\hat{D}_1^{x_2}$ term should be consistently taken into account; therefore we will keep $\hat{D}_1^{x_2}$ in the following data analysis.

As was discussed in our previously published paper,[10] the contribution of the $|\tau|^\beta$ term in eq 1 is dominant (larger than 95%).

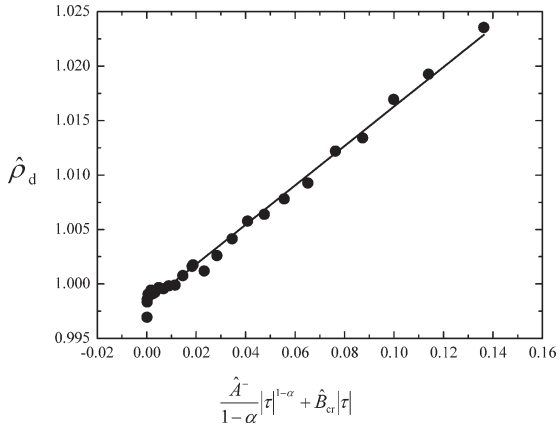

Figure 4. Plot of $\hat{\rho}_d$ versus $[\hat{A}^-/(1 - \alpha)]|\tau|^{1-\alpha} + \hat{B}_{cr}|\tau|$ for {benzonitrile + dodecane}: (●) the experimental values; solid line: the calculated values from eq 23.

To check the significance of the terms of the correction-to-scaling $|\tau|^{\Delta}$ and the asymmetry-related $|\tau|^{2\beta}$ in eq 1, we retained the two terms in a fitting procedure and compared it with that without them, and found that the changes in $\hat{B}_0^{x_2}$ and a_1 were less than 2% and 7%, respectively. Therefore we neglected the terms of $|\tau|^{\Delta}$ and $|\tau|^{2\beta}$ in eq 1 in the following fitting procedures.

From the points of view discussed above, we simplify eqs 1 and 2 to the forms:

$$\Delta Z_{\mathrm{cxc}} \equiv \frac{|Z^{\mathrm{U}} - Z^{\mathrm{L}}|}{2} \approx \pm \hat{B}_0^{Z}|\tau|^{\beta} \tag{21}$$

$$(x_2)_{\mathrm{d}} \equiv \frac{x_2^{\mathrm{U}} + x_2^{\mathrm{L}}}{2} \approx x_{2,\mathrm{c}} + \hat{D}_2^{x_2}|\tau|^{2\beta} + \hat{D}_1^{x_2}\left(\frac{\hat{A}^-}{1-\alpha}|\tau|^{1-\alpha} + \hat{B}_{\mathrm{cr}}|\tau|\right) \tag{22}$$

$$\hat{\rho}_{\mathrm{d}} \equiv \frac{\hat{\rho}^{\mathrm{U}} + \hat{\rho}^{\mathrm{L}}}{2} \approx \hat{\rho}_{\mathrm{c}} + \hat{D}_1^{\hat{\rho}}\left(\frac{\hat{A}^-}{1-\alpha}|\tau|^{1-\alpha} + \hat{B}_{\mathrm{cr}}|\tau|\right) \tag{23}$$

$$(\hat{\rho}x_2)_{\mathrm{d}} \equiv \frac{(\hat{\rho}x_2)^{\mathrm{U}} + (\hat{\rho}x_2)^{\mathrm{L}}}{2} \approx \hat{\rho}x_{2,\mathrm{c}} + \hat{D}_1^{\hat{\rho}x_2}\left(\frac{\hat{A}^-}{1-\alpha}|\tau|^{1-\alpha} + \hat{B}_{\mathrm{cr}}|\tau|\right) \tag{24}$$

and use them to analyze our experimental data in the next section.

Analysis of the Experimental Data with the Complete Scaling Formulation. In our previous works, we determined the $(T-x_2)$ coexistence curves for {benzonitrile + alkanes} and {dimethyl carbonate + alkanes} by measurements of the refractive indexes in two coexisting phases and the dependences of the refractive indexes on the temperature and the composition.[6−12] These $(T-x_2)$ coexistence curves were converted into $(T-\hat{\rho})$ and $(T-\hat{\rho}x_2)$ coexistence curves by $\hat{\rho} = V_{\mathrm{c}}/V$. Taking the assumption that the excess volume is negligible, then the molar volume V of the solution in the upper or lower phase or its critical value V_{c} is calculated by

$$V = (1-x_2)\frac{M_1}{d_1} + x_2\frac{M_2}{d_2} \tag{25}$$

separately, where d is the mass density, M is the molar mass, and the subscripts 1 and 2 represent the solvent and solute, respectively. The required values of d_i at various temperatures were obtained from the literature.[14,35,36]

The data of $(T-x_2)$, $(T-\hat{\rho})$ and $(T-\hat{\rho}x_2)$ coexistence curves were fitted by eq 21 to obtain the values of $\hat{B}_0^{x_2}$, $\hat{B}_0^{\hat{\rho}}$, and $\hat{B}_0^{\hat{\rho}x_2}$ for a series of binary solutions {benzonitrile + alkanes} and {dimethyl carbonate + alkanes}, which are listed in Table 6. In eqs 22, 23, and 24, the reduced critical amplitude of the heat capacity in the two-phase region $\hat{A}^-$ and the reduced critical background of the heat capacity $\hat{B}_{\mathrm{cr}}$ may be expressed by $\hat{A}^+/\hat{A}^- = 0.53$, $\hat{A}^+ = A^+V_{\mathrm{c}}/\alpha R$, and $\hat{B}_{\mathrm{cr}} = B_{\mathrm{cr}}V_{\mathrm{c}}/R$.[4,5] By using the values of A^+ and B_{cr} listed in Tables 3−5, the values $\hat{A}^-$ and $\hat{B}_{\mathrm{cr}}$ were calculated for all the systems studied and are also summarized in Table 5.

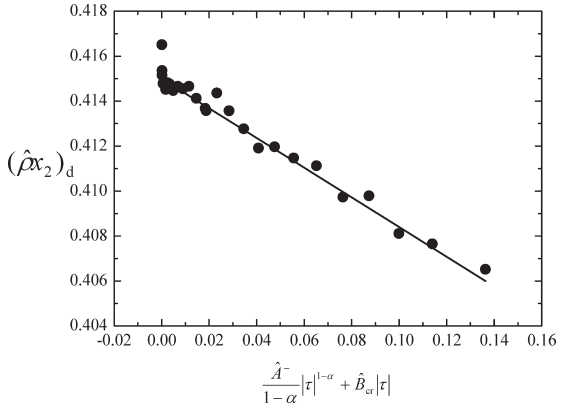

Figure 5. Plot of $(\hat{\rho}x_2)_{\mathrm{d}}$ versus $[\hat{A}^-/(1-\alpha)]|\tau|^{1-\alpha} + \hat{B}_{\mathrm{cr}}|\tau|$ for {benzonitrile + dodecane}: (●) the experimental values; solid line: the calculated values from eq 24.

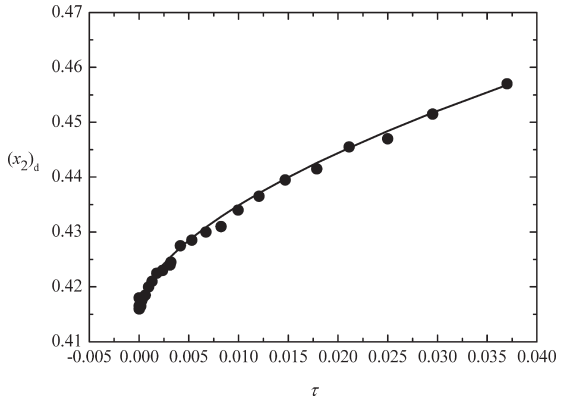

Figure 6. Plot of $(x_2)_{\mathrm{d}}$ vs τ for {benzonitrile + dodecane}. (●) the experimental values; solid line: the calculated values from eq 22.

In principle, the amplitudes $\hat{D}_1^{x_2}$ and $\hat{D}_2^{x_2}$ could be obtained by fitting the experimental data of the $(T-x_2)$ coexistence curve to eq 22; however, both the strong coupling between $|\tau|^{1-\alpha}$ and $|\tau|$ and the strong correlation between parameters $\hat{D}_1^{x_2}$ and $\hat{D}_2^{x_2}$ made the fit quite difficult. Therefore, an alternative procedure was taken. The experimental data of $(T-\hat{\rho})$ and $(T-\hat{\rho}x_2)$ coexistence curves were separately fitted by eqs 23 and 24 to obtain the values of $\hat{D}_1^{\hat{\rho}}$ and $\hat{D}_1^{\hat{\rho}x_2}$, which were substituted into eq 20 to obtain the value of $\hat{D}_1^{x_2}$. Equation 22 then was used to fit the experimental data of heat capacity and the coexistence curve $(T-x_2)$ to obtain $\hat{D}_2^{x_2}$ and $x_{2,\mathrm{c}}$. In each of the above three fitting procedures, besides the critical density Z_{c} (the correlation between Z_{c} and the other adjusting parameters is small), there was only one adjustable parameter, thus the correlations of the adjusting parameters were avoided. The values of $\hat{D}_1^{\hat{\rho}}$, $\hat{D}_1^{\hat{\rho}x_2}$ and $\hat{D}_2^{x_2}$ are listed in Table 6. The qualities of the fits were assessed by the values of χ^2 of the fits, which were all less than 0.35. As examples, Figures 4 −6 compare the experimental data with the fitting results for the solution {benzonitrile + dodecane} and show reasonably good consistency with each other. It may be found in Table 6 that the values of $\hat{D}_1^{x_2} = \hat{D}_1^{\hat{\rho}x_2} - \hat{D}_1^{\hat{\rho}}x_{2,\mathrm{c}}$ are system dependent and non-negligible, and their contribution to $\Delta x_{\mathrm{d}} \equiv (x_2^{\mathrm{U}} + x_2^{\mathrm{L}})/2 - x_{2,\mathrm{c}}$ ranges from 3% to 81%. The value of $x_{2,\mathrm{c}}$ as an adjusting parameter in eq 22 for each of the studied systems is listed and compared with that measured by the equal-volume technique[6−12] in Table 1.

dx.doi.org/10.1021/jp206380t |J. Phys. Chem. B 2011, 115, 13608–13616

Table 7. The Values of the Asymmetric Parameters a_1 Calculated by the Parameters Obtained from Fitting Widths and Diameters of the Coexistence Curves with eqs 21−24, and Calculated by the Parameters Obtained from Fitting the Diameters of the Coexistence Curves with eq 19, and Calculated by Theoretical eq 18 for Various Solute/Solvent Reduced Molar Volume Ratios $\hat{V}^0_{2,c}/\hat{V}^0_{1,c}$

system	$\hat{V}^0_{2,c}/\hat{V}^0_{1,c}$	a_1 (theory)	a_1(width)	a_1(dimeter)	a_1(fitting by eq 19)
BN[a] + C8[b]	1.578	−0.578	−0.576 ± 0.010	−0.61 ± 0.02	−0.17 ± 0.01
BN[a] + C9[c]	1.736	−0.736	−0.734 ± 0.002	−0.74 ± 0.01	−0.35 ± 0.01
BN[a] + C12[d]	2.217	−1.217	−1.216 ± 0.006	−1.23 ± 0.02	−0.73 ± 0.01
BN[a] + C14[e]	2.538	−1.538	−1.534 ± 0.005	−1.50 ± 0.03	−1.06 ± 0.01
BN[a] + C16[f]	2.857	−1.857	−1.853 ± 0.005	−1.81 ± 0.03	−1.39 ± 0.02
DMC[g] + C9[c]	2.126	−1.126	−1.128 ± 0.002	−1.10 ± 0.02	−0.92 ± 0.02
DMC[g]+ C10[h]	2.316	−1.316	−1.320 ± 0.003	−1.25 ± 0.02	−1.19 ± 0.02
DMC[g] + C12[d]	2.697	−1.697	−1.700 ± 0.004	−1.59 ± 0.02	−1.48 ± 0.02

[a] Benzonitrile. [b] Octane. [c] Nonane. [d] Dodecane. [e] Tetradecane. [f] Hexadecane. [g] Dimethyl carbonate. [h] Decane.

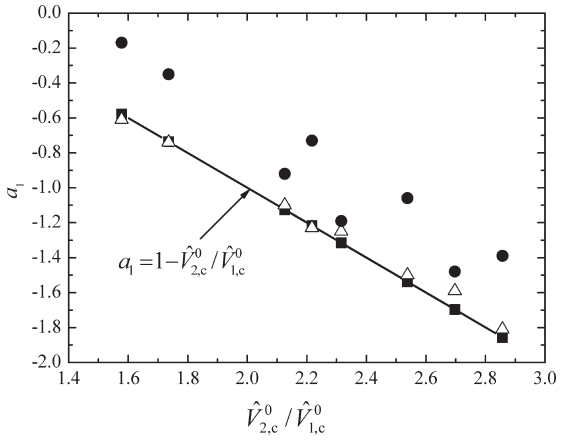

Figure 7. Plots of asymmetry coefficient a_1 against the solute/solvent reduced molar volume ratio $\hat{V}^0_{2,c}/\hat{V}^0_{1,c}$ at the critical temperature for all the studied systems: (●) asymmetry coefficients a_1 calculated from eq 27 by using amplitudes obtained by fitting eqs 19 and 21; (△) asymmetry coefficients a_1 calculated from eq 27 by using amplitudes obtained by fitting eqs 21−24; (■) asymmetry coefficients a_1 calculated from eq 26 by using amplitudes obtained by fitting eq 21; solid line: asymmetry coefficients a_1 calculated by $a_1 = 1 - \hat{V}^0_{2,c}/\hat{V}^0_{1,c}$.

The differences of the values of $x_{2,c}$ determined by the above two methods are less than 0.004, which is consistent with the estimated uncertainties introduced from the conversions of the refractive indexes to the mole fractions in measurements of the coexistence curves. Thus we conclude that eqs 22−24 are valid.

According to eqs 13 and 15 and taking $a_3 = 0$, the value of the asymmetry coefficient of coexistence curve a_1 can be calculated from the width and the diameter of the coexistence curve separately for each system we studied by

$$\frac{\hat{B}_0^{x_2}}{\hat{B}_0^{\rho}} = \frac{1 - a_1 x_{2,c}}{a_1} \tag{26}$$

$$\hat{D}_2^{x_2} = -\frac{a_1 (\hat{B}_0^{x_2})^2}{1 - a_1 x_{2,c}} \tag{27}$$

The calculated values of a_1 for a series of binary solutions together with various $\hat{V}^0_{2,c}/\hat{V}^0_{1,c}$ values are listed in Table 7. In order to evaluate the importance of the heat capacity for describing the asymmetry of the coexistence curves, we also calculated the values of a_1 from eq 27 by using the amplitudes obtained by simply fitting eqs 19 and 21 (the contribution of heat capacity was neglected), which are also listed in Table 7 for comparison. Figure 7 clearly shows that the values of a_1 determined from eq 27 by using the amplitudes obtained by fitting eqs 21−24 are more close to the values predicted by eq 18 than those by using the amplitudes obtained by fitting eq 19 and eq 21. It also can be seen from Figure 7 that the values of a_1 determined from eq 27 by using the amplitudes obtained by fitting eqs 21−24 and from eq 26 by using the widths of the coexistence curves are reasonably consistent with each other. It indicates that the heat capacity does play an important role for describing the asymmetric criticality of the coexistence curve.

■ CONCLUSIONS

The heat capacity per unit volume of the critical binary liquid solutions for {benzonitrile + octane, or dodecane, or hexadecane} and {dimethyl carbonate + nonane, or decane, or dodecane} have been measured over a wider temperature range both near and far away from the critical points by means of a differential scanning calorimeter. The exponents and amplitudes that characterize the heat capacity anomaly were obtained from the experimental data both in the one-phase and the two-phase regions, which were in accord with the theoretical predictions. The critical amplitudes of the correlation length were calculated by using the critical amplitudes of the heat capacity and the two-scale-factor universal ratio and found to be in agreement with the previously reported results. The universality of the ratio relating the critical amplitude of the heat capacity, the amplitude of the first correction to scaling term, and the critical background of the heat capacity was tested, and its value was found to be in agreement with the previously reported experimental results and that predicted by Anisimov, but significantly smaller than the theoretical prediction value of −0.708 proposed by Bagnuls and Bervillier. It was found that the value of the effective critical exponent of the heat capacity decreased from about 0.11 to almost zero as the distance from the critical point increased, indicating a critical crossover from the 3D-Ising to the mean-field. Furthermore, the experimental data of the heat capacity were used to study the asymmetry of the coexistence curves for systems {benzonitrile + alkanes} and {dimethyl carbonate + alkanes} in terms of the complete scaling theory proposed by Anisimov under incompressible conditions and neglecting the excess

volume. The results indicated that the heat capacity makes important contribution to the asymmetric behavior of the coexistence curves.

■ ASSOCIATED CONTENT

Supporting Information. The data of isobaric heat capacities per unit volume C_pV^{-1} of critical binary solutions {benzonitrile + octane, or dodecane, or hexadecane} and {dimethyl carbonate + nonane, or decane, or dodecane}. This material is available free of charge via the Internet at http://pubs.acs.org.

■ AUTHOR INFORMATION

Corresponding Author

*E-mail: shenwg@ecust.edu.cn. Tel.: +86 21 64250047. Fax: +86 2164252510.

Present Addresses

[§]Current address: Department of Basic Science, China Pharmaceutical University, Nanjing, Jiangsu 210009, China.

■ ACKNOWLEDGMENT

This work was supported by the National Natural Science Foundation of China (Projects 20973061, 21073063, and 21173080), the Chinese Ministry of Education (Key Project 105074), and the Committee of Science and Technology of Shanghai (Project 0652 nm010, 08JC1408100).

■ REFERENCES

(1) Fisher, M. E.; Orkoulas, G. *Phys. Rev. Lett.* **2000**, *85*, 696–699.
(2) Orkoulas, G.; Fisher, M. E.; Ustun, C. *J. Chem. Phys.* **2000**, *113*, 7530–7545.
(3) Cerdeiriña, C. A.; Anisimov, M. A.; Sengers, J. V. *Chem. Phys. Lett.* **2006**, *424*, 414–419.
(4) Wang, J. T.; Cerdeiriña, C. A.; Anisimov, M. A.; Sengers, J. V. *Phys. Rev. E.* **2008**, *77*, 031127.
(5) Perez-Sanchez, G.; Losada-Perez, P.; Cerdeiriña, C. A.; Sengers, J. V.; Anisimov, M. A. *J. Chem. Phys.* **2010**, *132*, 154502.
(6) Lei, Y. T.; Chen, Z. Y.; Wang, N.; Mao, C. F.; An, X. Q.; Shen, W. G. *J. Chem. Thermodyn.* **2010**, *42*, 864–872.
(7) Yin, T. X.; Lei, Y. T.; Huang, M. J.; Chen, Z. Y.; Mao, C. F.; An, X. Q.; Shen, W. G. *J. Chem. Thermodyn.* **2011**, *43*, 656–663.
(8) Huang, M. J.; Xiang, Y. S.; Chen, Z. Y.; Cai, L.; An, X. Q.; Shen, W. G. *J. Chem. Eng. Data* **2009**, *54*, 1477–1482.
(9) Mao, C. F.; Wang, N.; Peng, X. H.; An, X. Q.; Shen, W. G. *J. Chem. Thermodyn.* **2008**, *40*, 424–430.
(10) Huang, M. J.; Chen, Z. Y.; Yin, T. X.; An, X. Q.; Shen, W. G. *J. Chem. Eng. Data* **2011**, *56*, 2349–2355.
(11) Wang, N.; Mao, C. F.; Peng, X. H.; An, X. Q.; Shen, W. G. *J. Chem. Thermodyn.* **2006**, *38*, 732–738.
(12) Wang, J. S.; An, X. Q.; Wang, N.; Lv, H. K.; Chai, S. N.; Shen, W. G. *J. Chem. Thermodyn.* **2008**, *40*, 1638–1644.
(13) Cerdeiriña, C. A.; Miguez, J. A.; Carballo, E.; Tovar, C. A.; Tovar; De la Puente, E.; Romani, L. *Thermochim. Acta* **2000**, *347*, 37–44.
(14) Cibulka, I. *Fluid Phase Equilib.* **1993**, *89*, 1–18.
(15) Zabransky, M.; Ruzicka, V., Jr. *J. Phys. Chem. Ref. Data* **1990**, *19*, 719–762.
(16) Zabransky, M.; Ruzicka, V., Jr. *J. Phys. Chem. Ref. Data* **1991**, *20*, 405–444.
(17) Sengers, J. V.; Levelt-Sengers, J. M. H. *Progress in Liquid Physics*; Wiley: New York, 1978.
(18) Kumar, A.; Kishnamurthy, H. R.; Gopal, E. S. R. *Phys. Rep.* **1983**, *98*, 57–143.
(19) Tang, S.; Sengers, J. V.; Chen, Z. Y. *Phys. A (Amsterdam, Neth.)* **1991**, *179*, 344–377.
(20) Campostrini, M.; Pelissetto, A.; Rossi, P.; Vicari, E. *Phys. Rev. E* **1999**, *60*, 3526–3563.
(21) Bagnuls, C.; Bervillier, C.; Meiron, D. I.; Nickel, B. G. *Phys. Rev. B* **1987**, *35*, 3585–3607.
(22) Guida, R.; Zinn-Justin, J. *J. Phys. A: Math. Gen.* **1998**, *31*, 8103–8121.
(23) Parks, G. S.; Todd, S. S. *J. Chem. Phys.* **1934**, *2*, 440–441.
(24) Cerdeirina, C. A.; Tovar, C. A.; T., Gonalez-Sallgado, D.; Carballo, E.; Romani, L. *Phys. Chem. Chem. Phys.* **2001**, *3*, 5230–5236.
(25) Hasenbusch, M.; Pinn, K. *J. Phys. A* **1998**, *31*, 6157–6166.
(26) Bervillier, C.; Godreche, C. *Phys. Rev. B* **1980**, *21*, 5427–5431.
(27) Souto-Caride, M.; Wang, J. T.; Peleteiro, J.; Carballo, E.; Romani, L. *J. Therm. Anal. Calorim.* **2007**, *89*, 25–29.
(28) Souto-Caride, M.; Wang, J. T.; Peleteiro, J.; Carballo, E.; Romani, L. *Fluid Phase Equilib.* **2006**, *249*, 42–48.
(29) Bagnuls, C.; Bervillier, C. *Phys. Lett. A* **1985**, *107*, 299–304.
(30) Bagnuls, C.; Bervillier, C. *Phys. Lett. A* **1985**, *32*, 7209–7231.
(31) Anisimov, M. A.; Kiselev, S. B.; Sengers, J. V.; Tang, S. *Phys. A (Amsterdam, Neth.)* **1992**, *188*, 487–525.
(32) Anisimov, M. A.; Gorodetskii, E. E.; Kulikov, V. D.; Sengers, J. V. *Phys. Rev. E* **1995**, *51*, 1199–1215.
(33) Nicoll, J. F.; Albright, P. C. *Phys. Rev. B* **1986**, *34*, 1991–1996.
(34) Belyakov, M. Y.; Kiselev, S. B. *Phys. A (Amsterdam, Neth.)* **1992**, *190*, 75–94.
(35) Cibulka, I.; Takagi, T. *J. Chem. Eng. Data* **2002**, *47*, 1037–1070.
(36) Steele, W. V.; Chirico, R. D.; Knipmeyer, S. E.; Nguyen, A. *J. Chem. Eng. Data* **1997**, *42*, 1008–1020.